

# Production of bottomonium-like $Z_b$ states in $e-h$ and ultraperipheral $h-h$ collisions\*

Xiao-Yun Wang(王晓云)<sup>1†</sup> Wei Kou(寇维)<sup>2,3</sup> Qing-Yong Lin(林青勇)<sup>4‡</sup> Ya-Ping Xie(谢亚平)<sup>2,3§</sup>  
Xurong Chen(陈旭荣)<sup>2,3,5¶</sup> Alexey Guskov<sup>6‡</sup>

<sup>1</sup>Department of physics, Lanzhou University of Technology, Lanzhou 730050, China

<sup>2</sup>Institute of Modern Physics, Chinese Academy of Sciences, Lanzhou 730000, China

<sup>3</sup>University of Chinese Academy of Sciences, Beijing 100049, China

<sup>4</sup>Department of Physics, Jimei University, Xiamen 361021, China

<sup>5</sup>Guangdong Provincial Key Laboratory of Nuclear Science, Institute of Quantum Matter, South China Normal University, Guangzhou 510006, China

<sup>6</sup>Joint Institute for Nuclear Research, Dubna 141980, Russia

**Abstract:** The photoproduction of the bottomonium-like states  $Z_b(10610)$  and  $Z_b(10650)$  via  $\gamma p$  scattering is studied within an effective Lagrangian approach and the vector-meson-dominance model. The Regge model is employed to calculate the photoproduction of  $Z_b$  states via the  $t$ -channel with  $\pi$  exchange. The numerical results show that the values of the total cross-sections of  $Z_b(10610)$  and  $Z_b(10650)$  can reach 0.09 nb and 0.02 nb, respectively, near the center-of-mass energy of 22 GeV. Experimental measurements and studies of the photoproduction of  $Z_b$  states near the energy region around  $W \approx 22$  GeV are suggested. Moreover, with the help of eSTARlight and STARlight programs, we have obtained the cross-sections and numbers of events for  $Z_b(10610)$  production in electron-ion collisions (EIC) and ultraperipheral collisions (UPCs). The results show that a considerable number of  $Z_b(10610)$  events can be produced in the relevant experiments on EICs and UPCs. We have also calculated the rates and kinematic distributions for  $\gamma p \rightarrow Z_b n$  in  $ep$  and  $pA$  collisions via EICs and UPCs. The results will provide an important reference for the RHIC, LHC, EIC-US, LHeC, and FCC experiments in searching for bottomonium-like  $Z_b$  states.

**Keywords:** bottomonium-like states, electron-ion collisions, ultraperipheral collisions

**DOI:** 10.1088/1674-1137/abe3ec

## I. INTRODUCTION

In recent decades, with the continuous progress of high energy physics experiments, more and more exotic hadron states have been discovered [1-3]. The study of the production and properties of exotic hadron states is not only important for the improvement and development of the hadron spectrum and hadron classification, but is also of great significance for an in-depth understanding of non-perturbative quantum chromodynamics (QCD). The candidate particles of the exotic states that

have been discovered are mostly concentrated in the charm energy region, and the exotic states discovered in the bottom quark energy region are still very limited [1-3]. In 2011, two bottomonium-like states,  $Z_b(10610)$  and  $Z_b(10650)$ , were observed by the Belle Collaboration [4], and a series of subsequent experiments also discovered these two states from different decay channels [4-7]. Since the quantum numbers and decay properties of  $Z_b(10610)$  and  $Z_b(10650)$  are very similar [1], for convenience  $Z_b(10610)$  and  $Z_b(10650)$  will be abbreviated as  $Z_b$  in the following. These two states are considered to be

Received 18 September 2020; Accepted 8 February 2021; Published online 22 March 2021

\* This project is supported by the National Natural Science Foundation of China (12065014, 11705076, 11747160), and by the Strategic Priority Research Program of Chinese Academy of Sciences, (XDB34030301). This work is partly Supported by HongLiu Support Funds for Excellent Youth Talents of Lanzhou University of Technology. We also acknowledge the Natural Science Foundation of Fujian Province (2018J05007) and the Natural Science Foundation of Jimei University (ZQ2017007)

<sup>†</sup> E-mail: xywang@lut.edu.cn, Corresponding author

<sup>‡</sup> E-mail: qylin@jmu.edu.cn

<sup>§</sup> E-mail: xieyaping@impcas.ac.cn

<sup>¶</sup> E-mail: xchen@impcas.ac.cn

<sup>‡</sup> E-mail: avg@jinr.ru



Content from this work may be used under the terms of the Creative Commons Attribution 3.0 licence. Any further distribution of this work must maintain attribution to the author(s) and the title of the work, journal citation and DOI. Article funded by SCOAP<sup>3</sup> and published under licence by Chinese Physical Society and the Institute of High Energy Physics of the Chinese Academy of Sciences and the Institute of Modern Physics of the Chinese Academy of Sciences and IOP Publishing Ltd

different from traditional hadron states and are likely to contain at least four quarks [2,3].

Observations of the  $Z_b$  states have inspired extensive studies on the underlying properties, including interpretations as tetraquark states [8-11] and hadronic molecules [12-17]. More discussions can be found in Refs. [2,18]. In Ref. [3], the authors pointed out that since these two states were discovered through the decay reaction of bottomonium, the contribution of triangular singularities during the reaction cannot be neglected, which means that one cannot yet determine whether these two states are genuine particles. At present, investigating  $Z_b$  is still an interesting research topic.

Besides the analysis of the mass spectrum and the decay behavior, studying the production of  $Z_b$  by different mechanisms is very helpful to obtain definite evidence for their nature as genuine states. The meson photoproduction process has been proposed to be an effective way to search for exotic states [19-27]. We take notice of the  $Z_b \rightarrow \Upsilon(nS)\pi^+$  decay modes, which indicate that there exists a strong coupling between  $Z_b$  and  $\Upsilon(nS)\pi^+$ . Since  $\Upsilon(nS)$  is a vector meson, we suppose that we can produce the  $Z_b$  states through meson photoproduction. In the current work, the photoproduction of  $Z_b$  is studied within the framework of the effective Lagrangian approach and the vector-meson-dominance (VMD) model [28-30]. The calculations provide crucial information on a suitable process and the best energy window for searching for the  $Z_b$  states in related photoproduction experiments.

In hadron-hadron collisions, when the impact parameter between the two nuclei is larger than the sum of the radii of the two nuclei, the direct strong interaction between the nuclei is suppressed since the strong interaction is short range. However, the electromagnetic interaction cannot be neglected, since it is a long-range interaction. These collisions are called ultraperipheral collisions (UPCs) [31,32]. In UPCs, the photon is almost a real photon when the mass number of an atomic nucleus is larger than 16. Hence, UPCs are a good platform to study photoproduction with small photon virtuality.

Electron-ion colliders (EICs) are an important future platform to investigate nucleon structure. In an EIC, the electron scatters off a nucleon or nucleus via a virtual photon. Then, vector mesons and exotic states can be produced. Thus, the photoproduction of exotic states can be studied at EICs in the future. There are several proposed EIC plans, including the EicC, EIC-US, LHeC and FCC [33-36]. In EICs, the photon emitted from the electron beam has large virtuality. This is different from the photon in UPCs. Hence, EICs can be applied to investigate the photoproduction in a large  $Q^2$  region.

STARlight and eSTARlight are two important Monte Carlo packages to simulate the photoproduction of vector mesons and exotic states in UPCs and EICs [37-39]. The cross-sections of vector mesons and exotic states pro-

duced in photon-proton scattering are needed in the simulation process. Information about the four-momenta of final states is produced in the simulation processes. The total cross-sections of vector mesons or exotic states in UPCs and EICs are also calculated in STARlight and eSTARlight. In this work, the total cross-sections of  $Z_b$  at UPCs and the proposed EICs will be performed, using the STARlight and eSTARlight packages. The rapidity and transverse momentum distributions of  $Z_b$  will be presented. These distributions will be useful for the detector systems in future experiments.

This paper is organized as follows. We present the formalism for the production of  $Z_b$  in Section II. The numerical results for the  $Z_b$  production follow in Section III. Finally, the paper ends with a summary.

## II. FORMALISM

### A. $Z_b$ photoproduction in the $\gamma p \rightarrow Z_b n$ reaction

In this work, the production of the hidden-bottom  $Z_b(10610)$  and  $Z_b(10650)$  states via the  $\gamma p \rightarrow Z_b n$  reaction is studied with an effective Lagrangian approach. In the PDG book [1], one finds that  $Z_b(10610)$  or  $Z_b(10650)$  can decay to a bottomonium plus  $\pi$  meson with a branching ratio of a few percent. Since  $Z_b$  states are not directly coupled to photons, the VMD model can be used to calculate the photoproduction of  $Z_b$  states through the  $t$  channel with  $\pi$  exchange. The Feynman diagram of the  $\gamma p \rightarrow Z_b n$  reaction via  $t$  channel  $\pi$  exchange is depicted in Fig. 1. It is noted from Fig. 1 that we only consider the coupling of  $\Upsilon(1s, 2s, 3s)$  and photons. Also, although  $Z_b$  can also decay to  $h_b(1p, 2p)\pi$ , since the parity of the  $h_b$  state is opposite to that of the photon, the direct coupling of  $h_b$  to the photon can be neglected.

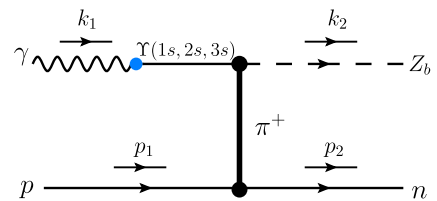


Fig. 1. (color online) Feynman diagram for the reaction  $\gamma p \rightarrow Z_b n$ .

#### 1. Lagrangians for the $Z_b$ production

In the PDG [1], the spin-parity quantum numbers of  $Z_b(10610)$  and  $Z_b(10650)$  are both  $1^+$ , and thus the Lagrangian densities for the vertices of  $Z_b \Upsilon \pi$  and  $\pi N N$  are written as [19,40],

$$\mathcal{L}_{Z_b \Upsilon \pi} = \frac{g_{Z_b \Upsilon \pi}}{M_{Z_b}} (\partial^\mu \Upsilon^\nu \partial_\mu \pi Z_{b\nu} - \partial^\mu \Upsilon^\nu \partial_\nu \pi Z_{b\mu}), \quad (1)$$

$$\mathcal{L}_{\pi NN} = -ig_{\pi NN} \bar{N} \gamma_5 \vec{\tau} \cdot \vec{\pi} N, \quad (2)$$

where  $Z_b$ ,  $\Upsilon$ ,  $\pi$  and  $N$  denote the fields of  $Z_b(10610)/Z_b(10650)$ ,  $\Upsilon$ , pion and nucleon meson, respectively. Here,  $g_{\pi NN}^2/4\pi = 12.96$  is adopted [41].

The coupling constant  $g_{Z_b \Upsilon \pi}$  can be derived from the corresponding decay width,

$$\Gamma_{Z_b \rightarrow \Upsilon \pi} = \left( \frac{g_{Z_b \Upsilon \pi}}{M_{Z_b}} \right)^2 \frac{|\vec{p}_\pi^{\text{c.m.}}|^2}{24\pi M_{Z_b}^2} \times \left[ \frac{(M_{Z_b}^2 - m_\Upsilon^2 - m_\pi^2)^2}{2} + m_\Upsilon^2 E_\pi^2 \right], \quad (3)$$

with

$$|\vec{p}_\pi^{\text{c.m.}}| = \frac{\lambda^{1/2}(M_{Z_b}^2, m_\Upsilon^2, m_\pi^2)}{2M_{Z_b}}, \quad (4)$$

$$E_\pi = \sqrt{|\vec{p}_\pi^{\text{c.m.}}|^2 + m_\pi^2}, \quad (5)$$

where  $\lambda$  is the Källén function with  $\lambda(x, y, z) \equiv \sqrt{(x-y-z)^2 - 4yz}$ , and  $M_{Z_b}$ ,  $m_\Upsilon$ , and  $m_\pi$  are the masses of  $Z_b$ ,  $\Upsilon$ , and the pion meson, respectively. The partial decay widths and coupling constants for  $Z_b \rightarrow \Upsilon \pi$  are listed in Table 1.

The coupling of  $Z_b$  to the photon can be derived using the VMD mechanism [28-30]. In the VMD mechanism, a real photon can fluctuate into a virtual vector meson, which subsequently scatters off the target proton.

The Lagrangian for the coupling of the meson  $\Upsilon$  with a photon reads as [24,25]

$$\mathcal{L}_{\Upsilon \gamma} = -\frac{em_\Upsilon^2}{f_\Upsilon} \Upsilon_\mu A^\mu, \quad (6)$$

where  $f_\Upsilon$  is the  $\Upsilon$  decay constant. Thus one gets the expression for the  $\Upsilon \rightarrow e^+ e^-$  decay width,

$$\Gamma_{\Upsilon \rightarrow e^+ e^-} = \left( \frac{e}{f_\Upsilon} \right)^2 \frac{8\alpha |\vec{p}_e^{\text{c.m.}}|^3}{3m_\Upsilon^2}, \quad (7)$$

where  $\vec{p}_e^{\text{c.m.}}$  denotes the three-momentum of an electron in the rest frame of the  $\Upsilon$  meson.  $\alpha = e^2/4\pi = 1/137$  is the

electromagnetic fine structure constant. With the partial decay width of  $\Upsilon(1S, 2S, 3S) \rightarrow e^+ e^-$  [1], one gets  $e/f_{\Upsilon(1S)} \simeq 0.008$ ,  $e/f_{\Upsilon(2S)} \simeq 0.005$  and  $e/f_{\Upsilon(3S)} \simeq 0.004$ .

## 2. Reggeized $t$ channel

Since the energy corresponding to the  $\gamma p \rightarrow Z_b n$  reaction is above 10 GeV, the Reggeized treatment will be applied to the  $t$  channel process. Usually, one just needs to replace the Feynman propagator with the Regge propagator as

$$\frac{1}{t - m_\pi^2} \rightarrow \left( \frac{s}{s_{\text{scale}}} \right)^{\alpha_\pi(t)} \frac{\pi \alpha'_\pi}{\Gamma[1 + \alpha_\pi(t)] \sin[\pi \alpha_\pi(t)]}, \quad (8)$$

where the scale factor  $s_{\text{scale}}$  is fixed at 1 GeV. In addition, the Regge trajectory of  $\alpha_\pi(t)$  is written as [40]

$$\alpha_\pi(t) = 0.7(t - m_\pi^2). \quad (9)$$

It can be seen that no free parameters have been added after introducing the Regge model.

## 3. Amplitude

Based on the Lagrangians above, the scattering amplitude for the reaction  $\gamma p \rightarrow Z_b n$  can be constructed as

$$-i\mathcal{M}_{\gamma p \rightarrow Z_b n} = \epsilon_{Z_b}^\mu(k_2) \bar{u}(p_2) \mathcal{A}_{\mu\nu} u(p_1) \epsilon_\nu(k_1), \quad (10)$$

where  $u$  is the Dirac spinor of the nucleon, and  $\epsilon_{Z_b}$  and  $\epsilon_\nu$  are the polarization vectors of the  $Z_b$  meson and photon, respectively.

The reduced amplitude  $\mathcal{A}_{\mu\nu}$  for  $t$ -channel  $Z_b$  photo-production reads

$$\mathcal{A}_{\mu\nu} = -i \left( \sqrt{2} g_{\pi NN} \frac{g_{Z_b \Upsilon \pi}}{M_{Z_b}} \frac{e}{f_\Upsilon} \right) \gamma_5 [k_1 \cdot (k_2 - k_1) g_{\mu\nu} - k_{1\mu} (k_2 - k_1)_\nu] \frac{1}{q^2 - m_\pi^2} \mathcal{F}_{\pi NN}(q^2) \mathcal{F}_{Z_b \Upsilon \pi}(q^2). \quad (11)$$

For the  $t$ -channel meson exchanges [19,20,23,40], the general form factor  $\mathcal{F}_t(q_t^2)$  consisting of  $\mathcal{F}_{Z_b \Upsilon \pi} = (m_\Upsilon^2 - m_\pi^2)/(m_\Upsilon^2 - q_\pi^2)$  and  $\mathcal{F}_{\pi NN} = (\Lambda_t^2 - m_\pi^2)/(\Lambda_t^2 - q_\pi^2)$  is taken into account. Here,  $q_\pi$  and  $m_\pi$  are the 4-momentum and mass of the  $\pi$  meson, respectively. The cutoff  $\Lambda_t$  will be taken as 0.7 GeV, which is the same as that in Ref. [19,21-23].

**Table 1.** The values of coupling constants  $g_{Z_b \Upsilon \pi}$  by taking the corresponding decay width of  $\Gamma_{Z_b \rightarrow \Upsilon \pi}$  in the PDG book [1]. The unit of width is MeV.

state	$\Gamma_{Z_b \rightarrow \Upsilon(1S)\pi}$	$g_{Z_b \Upsilon(1S)\pi}$	$\Gamma_{Z_b \rightarrow \Upsilon(2S)\pi}$	$g_{Z_b \Upsilon(2S)\pi}$	$\Gamma_{Z_b \rightarrow \Upsilon(3S)\pi}$	$g_{Z_b \Upsilon(3S)\pi}$
$Z_b(10610)$	0.099	0.487	0.662	3.299	0.386	9.292
$Z_b(10650)$	0.019	0.206	0.161	1.468	0.184	4.916

With the preparation in the previous sections, the differential cross section in the center of mass (c.m.) frame is written as

$$\frac{d\sigma}{d\cos\theta} = \frac{1}{32\pi s} \frac{|\vec{k}_2^{\text{c.m.}}|}{|\vec{k}_1^{\text{c.m.}}|} \left( \frac{1}{4} \sum_{\lambda} |\mathcal{M}|^2 \right). \quad (12)$$

Here,  $s = (k_1 + p_1)^2$ , and  $\theta$  denotes the angle of the outgoing  $Z_b$  meson relative to the  $\gamma$  beam direction in the c.m. frame.  $\vec{k}_1^{\text{c.m.}}$  and  $\vec{k}_2^{\text{c.m.}}$  are the three-momenta of the initial photon beam and final  $Z_b$  meson, respectively.

### B. $Z_b$ production in EIC and UPCs

In the electron-proton scattering, the cross-section of  $Z_b$  is given by [38,39]

$$\sigma(ep \rightarrow eZ_b n) = \int dk dQ^2 \frac{dN^2(k, Q^2)}{dk dQ^2} \sigma_{\gamma p \rightarrow Z_b n}(W, Q^2), \quad (13)$$

where  $k$  is the momentum of the photon emitted from the electron in the target rest frame,  $W$  is the c.m. energy of the photon and proton system, and  $Q^2$  is the virtuality of the photon. The photon flux reads as [42]

$$\frac{d^2 N(k, Q^2)}{dk dQ^2} = \frac{\alpha}{\pi k Q^2} \left[ 1 - \frac{k}{E_e} + \frac{k^2}{2E_e^2} - \left( 1 - \frac{k}{E_e} \right) \left| \frac{Q_{\text{min}}^2}{Q^2} \right| \right]. \quad (14)$$

The  $Q^2$  dependence of  $\sigma_{\gamma p \rightarrow Z_b n}(W, Q^2)$  is factorized as

$$\sigma_{\gamma p \rightarrow Z_b n}(W, Q^2) = \sigma_{\gamma p \rightarrow Z_b n}(W, Q^2 = 0) \left( \frac{M_V^2}{M_V^2 + Q^2} \right)^\eta, \quad (15)$$

where  $M_V$  is the mass of the vector meson. Since there is no parameter for the  $Z_b$  state, we apply the same  $\eta$  from  $J/\psi$  as Ref. [38]. This assumption has very little impact on the projection for  $Z_b$  because we consider  $0 < Q^2 < 1 \text{ GeV}^2$ , which gives quasi-real events [43].

The cross-section of an exotic charged particle in UPCs is computed in integrating the photon flux and photon-proton cross-section. The photon flux represents the number as a function of momentum of the photon emitted from a nucleus. In  $p$ - $A$  UPCs, the cross-section of  $pA \rightarrow nAZ_b$  reads [37]

$$\sigma(pA \rightarrow nAZ_b) = \int dk \frac{dN_\gamma(k)}{dk} \sigma_{\gamma p \rightarrow Z_b n}(W), \quad (16)$$

where  $k$  is the momentum of the real photon emitted from the nucleus, and  $W$  is the c.m. energy of the photon and proton system. The photon flux of the photon emitted from the nucleus is given as [44]

$$\frac{dN_\gamma(k)}{dk} = \frac{2Z^2\alpha}{\pi k} (XK_0(X)K_1(X) - \frac{X^2}{2}[K_1^2(X) - K_0^2(X)]), \quad (17)$$

where  $X = b_{\text{min}}k/\gamma_L$ , and  $b_{\text{min}} = R_A + R_p$  is the sum of the radii of the proton and nucleus.  $\gamma_L = \sqrt{s}/2m_p$  is the Lorentz boost factor.  $K_0(x)$  and  $K_1(x)$  are modified Bessel functions.  $Z$  denotes the charge number of the nucleus.

Adopting the cross-sections of  $Z_b$  in the photon-proton interaction, we can obtain the  $Z_b$  cross-sections in  $e$ - $p$  scattering in EIC and  $p$ - $A$  UPCs. With the help of the eSTARlight and STARlight packages, we can simulate the  $Z_b$  production processes and get the four-momenta of the final states. Then, we will further obtain  $Z_b$  in rapidity distributions and transverse momentum distributions, where the rapidity is defined as  $y = \frac{1}{2} \ln[(E + p_z)/(E - p_z)]$ .

## III. NUMERICAL RESULTS

### A. Photoproduction of $Z_b$

In Fig. 2 we present the total cross-sections for the reaction  $\gamma p \rightarrow Z_b n$ , from threshold to 50 GeV of the c.m. energy. One finds that the total cross-section of the  $\gamma p \rightarrow Z_b(10610)n$  scattering process reaches a maximum at the center-of-mass energy  $W \simeq 22$  GeV, which is about 0.09 nb. Also, when the cutoff parameter is changed from 0.5 to 0.9 GeV, the total cross-section of  $\gamma p \rightarrow Z_b(10610)n$  at  $W \simeq 22$  GeV is approximately between 0.06 and 0.12 nb.

### B. $Z_b$ production in EIC and UPCs

Photoproduction measurement is an important test of the structure of exotic states. Since the energy span of

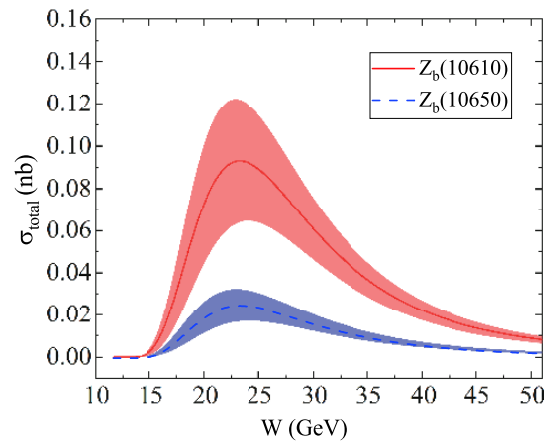


**Fig. 2.** (color online) Total cross-section for the  $\gamma p \rightarrow Z_b n$  reaction via pionic Regge trajectory exchange. The solid red and dashed blue lines are for  $Z_b(10610)$  and  $Z_b(10650)$  respectively. The value of cutoff  $\Lambda_r$  is taken as  $0.7 \pm 0.2$  GeV. The bands stand for the error bar of the cutoff  $\Lambda_r$ .

EIC and UPC facilities is large, it is advantageous to find the exotic states in the bottom quark energy region. Based on the previous  $Z_b$  photoproduction results, with the help of the eSTARlight and STARlight programs, we have obtained the cross-sections and numbers of events for  $Z_b(10610)$  production in EICs and UPCs. As presented in Table 2, the results were calculated based on several different accelerators. The cross-sections of  $Z_b(10610)$  in UPCs are larger than in EICs, since the photon flux of the nucleus is larger than the electron beam. However, the number of  $Z_b(10610)$  events in EICs is larger than that in UPCs, especially the FCC.

It can be seen from Table 2 that the differences between the total cross-sections in EICs are small, since the cross-section of EICs is not very sensitive to the collision energy. However, the cross-section of  $Z_b$  in EICs depends heavily on the value of the cross-section of  $Z_b$  photoproduction. It can be seen from Fig. 2 that if the c.m. energy is too small, the photoproduced cross-sections of  $Z_b$  will also be small, which indirectly leads to small cross-sections of  $Z_b$  in EICs. For the EicC [33], the present designation of collision energies is 5 GeV vs 20

GeV, so the c.m. energy is about 16.7 GeV. Thus, the cross-sections of  $Z_b(10610)$  in EicC will be very small. Table 3 shows the cross-sections of  $Z_b$  in EicC and the numbers of events when the beam energy is up to 10 GeV vs 100 GeV. These results will provide theoretical references for future experimental measurements and upgrades.

For  $Z_b(10610)$  production in EIC and UPC processes, we also present the rapidity distributions of  $Z_b(10610)$  in  $e-p$  and  $p-A$  processes, as shown in Fig. 3. These two distributions are relatively wide, which is related to the production mechanism of  $Z_b$  through the  $t$ -channel with pionic Regge trajectory exchange [23]. This indicates that the distribution shape of the rapidity and transverse momentum reflects the shape of the cross-section in Fig. 2. From the left-hand graph in Fig. 3, it can be seen that photoproduction at the EIC-US is near mid-rapidity and it is easy to identify in the detector system. From the right-hand graph of Fig. 3, we can also conclude that it is easier to observe  $Z_b(10610)$  in  $p$ -Au UPCs than in  $p$ -Pb UPCs, since the  $Z_b(10610)$  will be produced near mid-rapidity.

**Table 2.** Cross-sections and numbers of events for  $Z_b(10610)$  in  $e-p$  scattering and  $p-A$  UPCs. The integrated luminosities are the same as Ref. [42]. Luminosity of  $15 \times 10^{33} \text{ cm}^{-2} \text{ s}^{-1}$  was assumed for  $10^7 \text{ s}$  of running for the FCC [36].

	$e-p$ EIC-US	$e-p$ LHeC	$e-p$ FCC	$p$ -Au RHIC	$p$ -Pb LHC
Beam energy, GeV	18 ( $e$ ) vs. 275 ( $p$ )	60 ( $e$ ) vs. $7 \times 10^3$ ( $p$ )	60 ( $e$ ) vs. $50 \times 10^3$ ( $p$ )	100 ( $p$ ) vs. 100 (Au)	$7 \times 10^3$ ( $p$ ) vs. $2.778 \times 10^3$ (Pb)
Integrated luminosity	$10 \text{ fb}^{-1}$	$10 \text{ fb}^{-1}$	$150 \text{ fb}^{-1}$	$4.5 \text{ pb}^{-1}$	$2 \text{ pb}^{-1}$
$Z_b(10610)$ Cross sections	6.2 pb	8.5 pb	9.8 pb	2.0 nb	30 nb
Expected statistics, $10^6$ events	0.062	0.085	1.5	0.0090	0.060

**Table 3.** Cross-sections and numbers of events for  $Z_b(10610)$  in  $e-p$  collisions. Here, the integrated luminosity is taken as  $10 \text{ fb}^{-1}$ , which is the current design value of the EicC [33].

Beam energy	5 ( $e$ ) vs. 20 ( $p$ )	5 ( $e$ ) vs. 30 ( $p$ )	10 ( $e$ ) vs. 50 ( $p$ )	10 ( $e$ ) vs. 100 ( $p$ )
$Z_b(10610)$ cross sections	0.52 pb	1.3 pb	3.4 pb	4.4 pb
Expected statistics, $10^3$ events	5.2	13	34	44

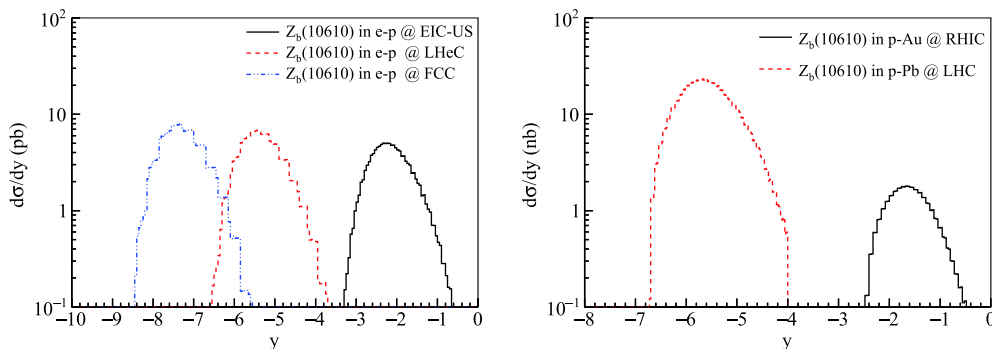


**Fig. 3.** (color online) Rapidity distributions of  $Z_b(10610)$  in (left)  $e-p$  at EIC-US, LHeC and FCC with  $0 < Q^2 < 1 \text{ GeV}^2$  and (right)  $p$ -Au and  $p$ -Pb UPCs at RHIC and LHC.

In addition, the transverse momentum distributions in  $e$ - $p$  scattering and  $p$ - $A$  UPCs are shown in Fig. 4. These results can be used as predictions for experiments. We notice that the three transverse momenta of the EICs are close to each other, since the total cross-sections are close to each other. These distributions can be employed to identify the exotic states. In  $p$ - $A$  UPCs, the difference between the two distributions is large because the total cross-section in  $p$ -Pb is larger than the cross-section in  $p$ -Au. It can be found that the largest value of transverse momentum is about 0.2 - 0.4 GeV in both EICs and UPCs.

We also give the  $t$ -distribution for  $Z_b(10610)$  production in  $e$ - $p$  and  $p$ - $A$  UPCs in Fig. 5. The  $t$ -distributions are close to each other in the three EICs and are different in the two UPCs. These conclusions are the same as for the transverse momentum distributions. Due to the adoption of the Regge propagator, it can be seen from Fig. 5 that the shape of the curves of the differential cross-sections of the  $t$ -distribution is relatively steep. This will be an important theoretical basis for us to clarify the role and contribution of the Regge propagator through EIC or UPC experiments.

#### IV. DISCUSSION AND SUMMARY

In this work, based on effective field theory and the

VMD mechanism, the photoproduction of the two bottomonium-like  $Z_b(10610)$  and  $Z_b(10650)$  states has been investigated for the first time. The numerical results show that the total cross-sections of the  $\gamma p \rightarrow Z_b n$  reaction reach a maximum at the center-of-mass energy  $W \approx 22$  GeV, which indicates that the center-of-mass energy 22 GeV is the best energy window for searching for the  $Z_b$  states via  $\gamma p$  scattering. Hence, an experimental study of the bottomonium-like states  $Z_b$  via the  $\gamma p$  reaction is suggested.

With the help of the eSTARlight and STARlight packages, the cross-sections and numbers of events for  $Z_b(10610)$  production in EICs and UPCs have been presented. As shown in Table 2, EIC experiments may collect more events due to their larger luminosity. Moreover, we have also simulated the rapidity and transverse momentum distributions of  $Z_b(10610)$  in  $e$ - $p$  scattering and  $p$ - $A$  UPC processes. These results will provide an important basis for estimating the production and studying the properties of  $Z_b$  in the RHIC, LHC, EIC-US, LHeC, and FCC in the future.

Since Reggeons are composed mostly of quarks, using Reggeons to probe the distributions of sea quarks and anti-quarks in nuclei may be a feasible method [39]. In this work, the photoproduction of  $Z_b$  is calculated by introducing the Regge exchange model. Thus, the numerical results will be beneficial for experimental studies of the

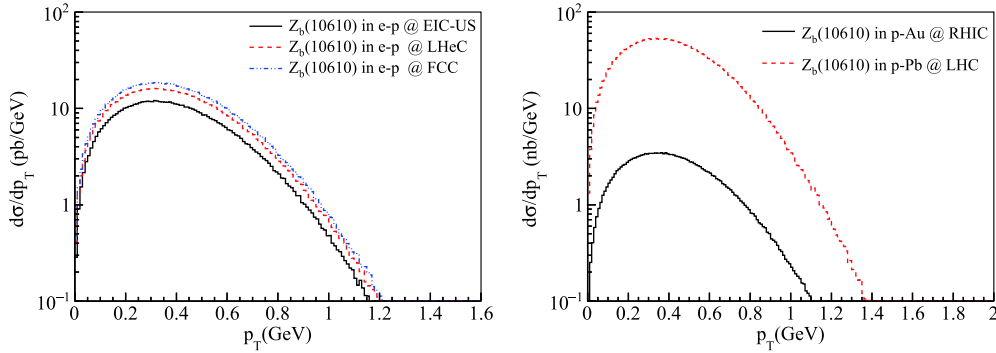


Fig. 4. (color online) Transverse momentum distributions of  $Z_b(10610)$  in (left)  $e$ - $p$  at EIC-US, LHeC and FCC with  $0 < Q^2 < 1 \text{ GeV}^2$  and  $p$ -Au and  $p$ -Pb UPCs at RHIC and LHC

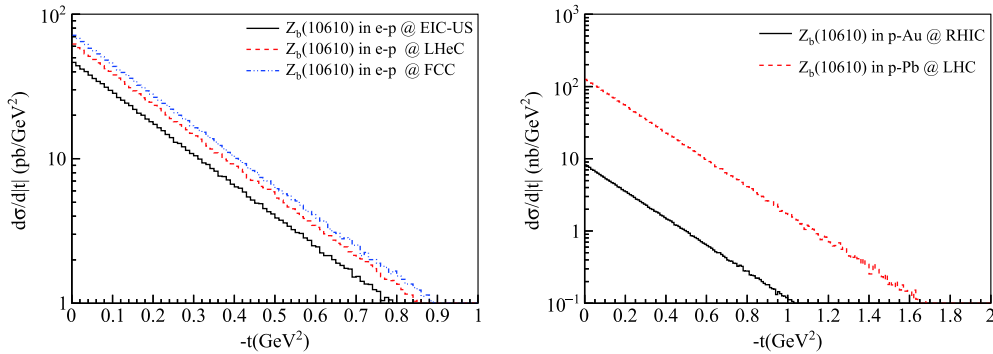


Fig. 5. (color online)  $t$ -distributions for  $Z_b(10610)$  production in (left)  $e$ - $p$  and  $p$ - $A$  scattering.

Reggeon model. Also, the cross-sections of  $t$  distributions of  $Z_b$  in different scattering processes have been ob-

tained, which will provide an important theoretical reference for clarifying the role and contribution of Reggeons.

## References

- [1] M. Tanabashi *et al.* (Particle Data Group), *Phys. Rev. D* **98**, 030001 (2018)
- [2] Y. R. Liu, H. X. Chen, W. Chen *et al.*, *Prog. Part. Nucl. Phys.* **107**, 237-320 (2019)
- [3] F. K. Guo, X. H. Liu, and S. Sakai, *Prog. Part. Nucl. Phys.* **112**, 103757 (2020)
- [4] A. Bondar *et al.* (Belle Collaboration), *Phys. Rev. Lett.* **108**, 122001 (2012)
- [5] I. Adachi *et al.* (Belle Collaboration), arXiv: 1105.4583; arXiv: 1209.6450
- [6] A. Garmash *et al.* (Belle Collaboration), *Phys. Rev. Lett.* **116**, 212001 (2016)
- [7] A. Garmash *et al.* (Belle Collaboration), *Phys. Rev. D* **88**, 052016 (2013)
- [8] A. Ali, C. Hambrock, and W. Wang, *Phys. Rev. D* **85**, 054011 (2012), arXiv:1110.1333[hep-ph]
- [9] A. Esposito, A. L. Guerrieri, F. Piccinini *et al.*, *Int. J. Mod. Phys. A* **30**, 1530002 (2015), arXiv:1411.5997 [hep-ph]
- [10] L. Maiani, A. Polosa, and V. Riquer, *Phys. Lett. B* **778**, 247-251 (2018), arXiv:1712.05296[hep-ph]
- [11] Z. G. Wang and T. Huang, *Nucl. Phys. A* **930**, 63-85 (2014)
- [12] A. Bondar, A. Garmash, A. Milstein *et al.*, *Phys. Rev. D* **84**, 054010 (2011), arXiv:1105.4473[hep-ph]
- [13] J. R. Zhang, M. Zhong, and M. Q. Huang, *Phys. Lett. B* **704**, 312-315 (2011), arXiv:1105.5472[hep-ph]
- [14] Z. F. Sun, J. He, X. Liu *et al.*, *Phys. Rev. D* **84**, 054002 (2011), arXiv:1106.2968[hep-ph]
- [15] H. W. Ke, X. Q. Li, Y. L. Shi *et al.*, *JHEP* **04**, 056 (2012), arXiv:1202.2178[hep-ph]
- [16] J. Dias, F. Aceti, and E. Oset, *Phys. Rev. D* **91**, 076001 (2015), arXiv:1410.1785[hep-ph]
- [17] Q. Wang, V. Baru, A. Filin *et al.*, *Phys. Rev. D* **98**, 074023 (2018), arXiv:1805.07453[hep-ph]
- [18] F. K. Guo, C. Hanhart, U. G. Meiuier *et al.*, *Rev. Mod. Phys.* **90**, 015004 (2018), arXiv:1705.00141[hep-ph]
- [19] X. H. Liu, Q. Zhao, and F. E. Close, *Phys. Rev. D* **77**, 094005 (2008)
- [20] J. He and X. Liu, *Phys. Rev. D* **80**, 114007 (2009)
- [21] G. Galata, *Phys. Rev. C* **83**, 065203 (2011)
- [22] Q. Y. Lin, X. Liu, and H. S. Xu, *Phys. Rev. D* **88**, 114009 (2013)
- [23] X. Y. Wang, X. R. Chen, and A. Guskov, *Phys. Rev. D* **92**, 094017 (2015)
- [24] X. Y. Wang, X. R. Chen, and J. He, *Phys. Rev. D* **99**, 114007 (2019)
- [25] X. Y. Wang, J. He, and X. Chen, *Phys. Rev. D* **101**, 034032 (2020)
- [26] Y. P. Xie, X. Y. Wang, and X. Chen, *Chin. Phys. C* **45**, 014107 (2021)
- [27] M. Albaladejo *et al.* (JPAC), *XYZ spectroscopy at electron-hadron facilities: Exclusive processes*, arXiv: 2008.01001 [hep-ph]
- [28] T. H. Bauer, R. D. Spital, D. R. Yennie, and F. M. Pipkin, *Rev. Mod. Phys.* **50**, 261 (1978) Erratum: [*Rev. Mod. Phys.* **51**, 407 (1979)] doi:10.1103/RevModPhys.50.261
- [29] T. Bauer and D. R. Yennie, *Phys. Lett. B* **60**, 165 (1976)
- [30] T. Bauer and D. R. Yennie, *Phys. Lett. B* **60**, 169 (1976)
- [31] C. A. Bertulani, S. R. Klein, and J. Nystrand, *Ann. Rev. Nucl. Part. Sci.* **55**, 271-310 (2005), arXiv:nucl-ex/0502005[nucl-ex]
- [32] A. J. Baltz, G. Baur, D. d'Enterria *et al.*, *Phys. Rept.* **458**, 1-171 (2008), arXiv:0706.3356[nucl-ex]
- [33] X. Chen, *PoS DIS* **2018**, 170 (2018), arXiv:1809.00448[nucl-ex]
- [34] C. Montag, Presented at the EIC Users Group Meeting 2017, Trieste, Italy, (2017)
- [35] J. L. Abelleira Fernandez *et al.* (LHeC Study Group), *J. Phys. G* **39**, 075001 (2012)
- [36] F. Bordry, M. Benedikt, O. Brning *et al.*, arXiv: 1810.13022 [physics.acc-ph]
- [37] S. R. Klein, J. Nystrand, J. Seger *et al.*, *Comput. Phys. Commun.* **212**, 258-268 (2017)
- [38] M. Lomnitz and S. Klein, *Phys. Rev. C* **99**, 015203 (2019)
- [39] S. R. Klein and Y. P. Xie, *Phys. Rev. C* **100**, 024620 (2019)
- [40] X. Y. Wang, J. He, X. R. Chen *et al.*, *Phys. Lett. B* **797**, 134862 (2019)
- [41] Z. W. Lin, C. M. Ko, and B. Zhang, *Phys. Rev. C* **61**, 024904 (2000)
- [42] V. M. Budnev, I. F. Ginzburg, G. V. Meledin *et al.*, *Phys. Rept.* **15**, 181 (1975)
- [43] O. Gryniuk, S. Joosten, Z. E. Meziani *et al.*, arXiv: 2005.09293 [hep-ph]
- [44] S. Klein and J. Nystrand, *Phys. Rev. C* **60**, 014903 (1999), arXiv:hep-ph/9902259